Morphological Transformations and Fusion of PbSe Nanocrystals Studied Using Atomistic Simulations

ARTICLE *in* NANO LETTERS · OCTOBER 2010

Impact Factor: 13.59 · DOI: 10.1021/nl101793b · Source: PubMed

5 AUTHORS, INCLUDING:

Philipp Schapotschnikow
Brains for hire
12 PUBLICATIONS **366** CITATIONS
SEE PROFILE

Marijn van Huis
Utrecht University
112 PUBLICATIONS **1,603** CITATIONS
SEE PROFILE

Henny Zandbergen
Delft University of Technology
668 PUBLICATIONS **18,354** CITATIONS
SEE PROFILE

Daniel Vanmaekelbergh
Utrecht University
291 PUBLICATIONS **10,639** CITATIONS
SEE PROFILE

NANO LETTERS

pubs.acs.org/NanoLett

Morphological Transformations and Fusion of PbSe Nanocrystals Studied Using Atomistic Simulations

Philipp Schapotschnikow,[†,⊥] Marijn A. van Huis,[*,‡,§] Henny W. Zandbergen,[‡] Daniël Vanmaekelbergh,[∥] and Thijs J. H. Vlugt[†]

[†] Process and Energy Laboratory, Delft University of Technology, Leeghwaterstraat 44, 2628 CA Delft, The Netherlands, [‡] Kavli Institute of Nanoscience, Delft University of Technology, Lorentzweg 1, 2628 CJ Delft, The Netherlands, [§] EMAT, University of Antwerp, Groenenborgerlaan 171, 2020 Antwerp, Belgium, and [∥] Debye Institute for NanoMaterials Science, Utrecht University, Princetonplein 1, 3508 TH Utrecht, The Netherlands

ABSTRACT Molecular dynamics simulations are performed on capped and uncapped PbSe nanocrystals, employing newly developed classical interaction potentials. Here, we show that two uncapped nanocrystals fuse efficiently via direct surface attachment, even if they are initially misaligned. In sharp contrast to the general belief, interparticle dipole interactions do not play a significant role in this "oriented attachment" process. Furthermore, it is shown that presumably polar, capped PbSe{111} facets are never fully Pb- or Se-terminated.

KEYWORDS Nanocrystal fusion, PbSe, polar surfaces, molecular dynamics, force field

The field of nanoscience has rapidly evolved from the study of isolated nanocrystals (NCs) to the fabrication and manipulation of mesoscale nanomaterials,[1] which can be either two- or three-dimensional arrays of (heterogeneous) nanocrystals,[2−5] or continuous nanostructures with complex dimensional configurations such as nanowires formed by oriented attachment of nanocrystals.[6−8] Single, isolated PbSe NCs display peculiar electronic and optoelectronic properties such as strong quantum confinement, and multiexciton generation.[9] Assemblies made of PbSe nanocrystals feature in IR photon detectors[10−12] and in nanocrystal thin-film transistors.[13] Furthermore, PbSe nanocrystals show a remarkable propensity for crystal unification and have therefore been used as building units for the synthesis of larger nanostructures such as nanorods, nanorings, and nanostars.[3,6,14,15] The process of fusion of (initially) randomly oriented nanocrystals into larger single crystals is commonly referred to as "oriented attachment".[14,16,17] Recently, the mechanism of crystal fusion was observed in real time during in situ heating in a high-resolution transmission electron microscope (HRTEM).[16] Upon heating, surfactant molecules are removed from the surface, and after initial attachment rotations of the nanocrystals over multiple axes enable crystal fusion.

Dipolar interactions[18,19] between the NCs are presumed to play an important role in the fusion process, although direct experimental evidence is lacking. This assumption is based on the argument that a random distribution of polar {111} facets generates a permanent electric dipole moment (of variable strength) in multifaceted NCs with a rocksalt crystal structure.[14] However, recent first-principles calculations[20] suggest that energetically very favorable reconstructions render the {111} surfaces much less polar, which implies that surface energy may play a more prominent role than is currently presumed.

Molecular simulations with classical potentials can be used to elucidate the relevant physical mechanisms behind the efficient oriented attachment. In contrast to HRTEM experiments, there is no influence from any supporting substrate, the exact ligand coverage of the NCs at any moment is known, and dipole moments can be computed directly during the simulation. In the past, useful insights have been obtained with classical atomistic simulations performed on bare and ligand-covered CdSe nanocrystals.[21−23] Since no force fields for PbSe were available thus far, we derive the potentials in the present work. Next, we investigate by means of molecular dynamics simulations the mechanical and energetic stability of (ligand-covered) facets, including the presumably polar {111} facets, and the nanocrystal fusion mechanism of initially aligned and misaligned PbSe nanocrystals. We consider ethylamine as the capping agent in the present work because (i) alkylamines are commonly used in investigations of the oriented crystal attachment of PbSe NCs[16,20] and (ii) they have a well-defined chemical state, unlike carboxylic (or phosphonic) acids or thiols.

* To whom correspondence should be addressed. Tel. +31 15 2782272. E-mail: m.a.vanhuis@tudelft.nl.

[⊥] Present address: Dacolt International BV, Oxfordlaan 70, 6229 EV Maastricht, The Netherlands.

Received for review: 05/21/2010
Published on Web: 09/16/2010

TABLE 1. Computed and Experimental Lattice Parameters and Elastic Constants of PbSe in the Rocksalt (NaCl), CsCl, and Zincblende (ZB) Crystal Structures[a]

	present model	QM (literature)	experiment (literature)
a (NaCl) [Å]	6.06 (0 K) 6.10 (300 K)	**6.05**[f]; 6.20[f]; 6.10[g]; 6.21[e]; 6.23−6.27[b]	6.11[d],6.13[c]
a (CsCl) [Å]	3.66 (0 K) 3.40 (300 K, 30 GPa)	**3.67**[f], 3.77[e]	3.38[c] (300 K, 30.3 GPa)
a (ZB) [Å]	6.77	6.88[f]	
B (NaCl) [GPa]	54.3	58.3[f]; 49.1[f]; 60.8[g]; 49.5[e]; 44.5−48.3[b]	**54.1**[h]
B (CsCl) [GPa]	60.4	63.0[f]; 62.0[e]	
B (ZB) [GPa]	36.7	32.0[f]	
C_{11} [GPa]	124.7	160[f]; 121[f]	**123.7**[h]
C_{21} [GPa]	19.02	7.8[f]; 8.9[f]	**19.3**[h]
C_{44} [GPa]	19.02	18.0[f]; 17.2[f]	**15.9**[h]

[a] All QM calculations were performed for zero pressure conditions and for a temperature of 0 K. The experimental data were obtained at room temperature and at ambient pressure, except for the CsCl lattice parameter obtained at a pressure of 30.3 GPa. The values in bold face were used for fitting the potential. [b] Reference 27. [c] Reference 28. [d] Reference 29. [e] Reference 30. [f] Reference 31. [g] Reference 32. [h] Reference 33.

We have developed interatomic potentials for PbSe within an interaction model that (i) has a minimum number of fitting parameters, (ii) reproduces the properties of bulk PbSe in the solid state, and (iii) can be straightforwardly combined with atomistic interaction models for ligand and solvent molecules. The approach of classical force fields is used, whereby the interaction between the atoms is described by a sum of Lennard-Jones (LJ) and Coulomb potentials

$$U_{ij}(r_{ij}) = U_{\text{Coulomb}}(r_{ij}) + U_{\text{LJ}}(r_{ij}) = \frac{q_i q_j}{4\pi\varepsilon_0 r_{ij}} + 4\varepsilon_{ij}\left[\left(\frac{\sigma_{ij}}{r_{ij}}\right)^{12} - \left(\frac{\sigma_{ij}}{r_{ij}}\right)^{6}\right] \quad (1)$$

Here r_{ij} is the distance between atoms i and j; ε_{ij} and σ_{ij} are the LJ parameters; q_i and q_j are partial charges on atoms i and j; and ε_0 is the dielectric constant of vacuum. To reduce the number of independent interaction parameters, only the LJ coefficients for the atoms of the same type are usually defined. The remaining cross-coefficients are then obtained from the Lorentz−Berthelot mixing rules. We apply the united atom model for ethylamine capping molecules (NC2), where CH_2 and CH_3 groups are represented by single pseudoatoms. The N atoms are modeled explicitly, and amine H atoms are modeled as point charges. Atoms of the same molecule interact via bond stretching, bond bending, and torsional forces. Atoms of different molecules interact via the Coulomb and LJ potentials eq 1. The parameters for the intra- and intermolecular interactions for NC2 are taken from the TraPPE force field.[24] The five interaction parameters for PbSe (four LJ coefficients and the partial charge) were fitted to the available elastic and lattice constants using the GULP code.[25,26] The fitted parameters are given in the Supporting Information.

In Table 1, the lattice parameters and elastic constants calculated using our potentials are compared with the corresponding experimental values and results of quantum mechanical (QM) computations from literature. All values are in excellent agreement, even for the properties that were not used for the development of the model (see caption of Table 1). It is important to note that the QM calculations are performed at zero-temperature and zero-pressure conditions, and therefore they do not account for thermal effects such as expansion and softening. Thus, it is natural to compare our calculation results at 0 K to the QM data, and our calculations at 300 K to the experimental measurements. The computed pressure−enthalpy diagram for bulk PbSe in different crystal structures is also in good agreement with experiment (details in the Supporting Information).

In the molecular dynamics (MD) simulations, the equations of motion were integrated using the velocity Verlet algorithm with a time step of 2 fs. Details of the simulation settings are given in the Supporting Information. Our main attention is focused on a multifaceted nanocrystal in the commonly observed morphology, as shown in Figure 1 (bottom left).[20] To generate such structure, a cube is cut out from a bulk PbSe lattice with rocksalt crystal structure, and this cube is truncated at corners and edges. The resulting NC consists of 672 atoms, has a diameter of 3.4 nm, and exposes {100}, {110}, and {111} facets. Next, 214 ethylamine-capping molecules are added to this structure without allowing for the movement of atoms in the NC. This is done using a grand-canonical Monte Carlo (MC) simulation at 300 K (details in the Supporting Information). The resulting capped structure is showed in Figure 1 (left). The number of capping molecules is larger than the number of surface Pb atoms (132) but is smaller than the number of dangling bonds on Pb atoms (264). It is not possible to passivate all missing bonds, since steric hindrance prevents three amine molecules from adsorbing to the same surface cation on a {111} facet.

First, the importance of the capping molecules for the mechanical stability of faceted NC morphologies is investigated. To release the surface strain, we run a gradient descent optimization (GDO, equivalent to MD at 0 K) of the multifaceted NC with or without ligands with the purpose

DOI: 10.1021/nl101793b | *Nano Lett.* **2010,** *10,* 3966–3971

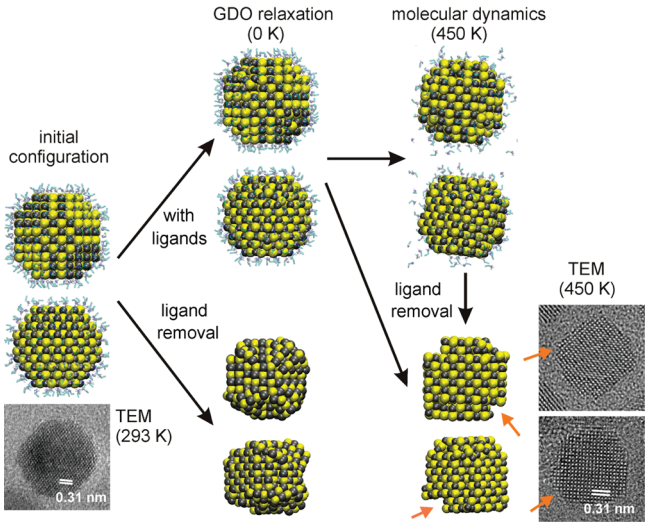

FIGURE 1. Simulation of relaxation and annealing of multifaceted PbSe NCs with a size of 3.4 nm, $\{PbSe\}_{336}$. Each structure is shown in the [100] (upper image) and [110] (lower image) projections. The Pb and Se atoms are represented by black and yellow spheres, respectively; blue lines represent NC2 capping molecules. The starting configuration is shown on the left, simulations with ligands on top and simulations without ligands at the bottom. Black arrows pointing downward imply removal of ligands before the simulation. The initial morphology is relaxed through a GDO optimization (MD at 0 K), which yields the structures at the center. The structures on the right are obtained from a MD simulation at 450 K. The experimental TEM images[20] are obtained from as-dropcast nanocrystals (bottom left, [110] projection) and after annealing to a temperature of 450 K for 30 min (bottom right, [100] projection). Short, orange arrows indicate {100} nanofringes.

of reaching the closest local potential energy minimum. If the NC undergoes a significant structural transformation to reach such a minimum, it is a clear sign that the initial morphology is mechanically unstable due to a structural strain. Figure 1 (top center) shows the capped NC after strain relaxation. The structures before and after relaxation are very similar. It is of importance to note that all facets remain intact. Close inspection shows that the {111} facets in the relaxed structure are not purely Pb or Se terminated, but that some atoms of the subsurface layers have migrated to the surface. Thus in contrast to what is generally assumed in the literature, the facets are not terminated by a single, perfectly smooth atomic layer. Another interesting observation is that the structure remains symmetrical. This is nontrivial since the amine ligands bind primarily to cations, so that the surface anions are not passivated.

In contrast with the capped NCs, a bare NC is unstable in the faceted morphology. Figure 1 (bottom center) shows a NC after strain relaxation without capping molecules. The drastic reconstructions in the {111} direction shows that the initial morphology is mechanically unstable, implying that much tension is present in the bare, multifaceted morphology due to the presence of facets different from the {100}-type. Because ligand-covered, multifaceted NCs are mechanically stable, it can be concluded that the capping molecules significantly reduce the surface tension caused by polar facets.

We proceed by studying the energetic stability, thereby mimicking experimental conditions. During an in situ TEM experiment,[20] it was observed that upon annealing at a temperature of 450 K, the ligands evaporate from the NC surface. During this process, the morphology of the NCs changes from multifaceted to cubic, whereby the {110}- and {111}-type facets have reconstructed into tiny {100} fringes. The very beginning of the TEM experiment is simulated using the capped relaxed NCs (Figure 1 top center) as initial structures. We carry out a MD simulation of 20 ns at a temperature of 450 K, out of which the first 1 ns serves equilibration. We observe that after a few hundred picoseconds, some ligand molecules begin to come off from the NC surface and move into the gas phase inside the simulation box. After a few nanoseconds, an equilibrium between the NC surface and the surrounding gas phase is established with frequent adsorption and desorption events. At the same time, surface reconstruction takes place. In particular, the polar {111} facets are affected by this reconstruction: atoms from the subsurface layers migrate into the outer layer. As a result, the surface of the {111} facets changes into a configuration with irregularly distributed Pb and Se adatoms on top of the surface, see Figure 1 (top right). One can also clearly see that the {110} facets remain fully intact. Because TEM can only visualize rows of atoms and not individual atoms, such a NC would be recognized as a regular multifaceted NC under TEM.

Next, we simulate the second stage of the TEM experiment, where the ligands have eventually all evaporated from the surface. Considering that the amine ligands begin to desorb from the surface already after a few hundred picoseconds, it is reasonable to assume that after a few nanoseconds the vast majority will have evaporated. We realize this situation by taking the NC core from a simulation with ligands as initial configuration but without including the ligand molecules (otherwise, these would always readsorb from the gas phase because of the periodic boundary conditions in the simulation). The final structure is shown in Figure 1 (bottom right). In contrast to the capped NC, the {111} facets disappear entirely; steps and fringes form instead. Both the transformation into a cubic NC morphology, and the formation of the {100}-nanofringes in the simulation are in excellent agreement with the experimental TEM observations.[20] A few representative TEM images are included at the right-hand side of Figure 1.

The potential energy of the NC, during the transformation of multifaceted to cubic, decreases upon annealing. However, both the number of surface atoms (ca. 350) and the number dangling bonds (ca. 600) are increased by more than a factor two in comparison with the initial configuration. This means that the potential energy of a specific morphology is not solely determined by the area of its surface or by the number of dangling bonds; there is a large

DOI: 10.1021/nl101793b | *Nano Lett.* **2010,** *10,* 3966–3971

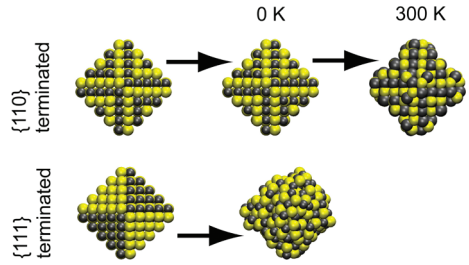

FIGURE 2. Relaxation and annealing of PbSe NC in two different octahedral morphologies. Representations as in Figure 1. Top: the octahedron is obtained by truncating a cube in the (110) directions at the edge midpoints. Bottom: the octahedron is obtained by truncating a cube in the (111) directions at the edge midpoints.

contribution to the surface energy from the subsurface layers. The questions now arises which facets mainly contribute to the observed mechanical instability of bare multifaceted NCs, the {111}-type facets or the {110}-type facets. To investigate the influence of the different types of facets, a relaxation study was performed on PbSe NCs having only {100}-, only {110}-, or only {111}-type facets. Cubic, fully {100}-terminated NCs are mechanically stable; A GDO of a bulk PbSe cube leads to a slight contraction of surface bonds (1−2%) without any structural changes (not shown). To study the mechanical stability of {110} and {111} facets, respectively, we consider two octahedral morphologies as shown in Figure 2 (left). The first morphology is the "classical" octahedron that is obtained by truncating a cube in all {111} directions at the edge midpoints. This structure has purely Pb (or Se) terminated facets. The second morphology is constructed by truncating a cube along all the {110} directions at the edge midpoints. Its facets have the shape of a step pyramid with alternating anion and cation layers. Although this structure looks like an octahedron, it is {110} terminated. The GDO shows that the first structure, the {111}-terminated octahedron, is mechanically unstable, while the {110}-terminated octahedron is mechanically stable.

This is of importance for the understanding of the electrostatic properties of octahedral PbSe NCs, as the {110} facets are not polar while the {111} facets are. We can conclude that any morphology with purely anion or cation terminated {111} facets is subject to structural strain. This strain can be relaxed in three (not mutually exclusive) ways: (i) passivation with appropriate ligands, (ii) formation of mixed-terminated structures including ad-atoms and ad-rows,[20] islands, and step pyramids, and (iii) structural transformation leading to elimination of {111} facets.

In a MD simulation at 300 K, the {110}-terminated octahedron slowly transforms into a star with tips along the {100} directions, see Figure 2 (right). We have made similar observations for cubic NCs truncated in the {110} directions. Note that these shapes (multifaceted, octahedral, starlike) are well-known from experimental work on PbSe NCs; and the stability of individual morphology depends in a very sensitive way on the ligands present in the reaction mixture during synthesis.[6,15]

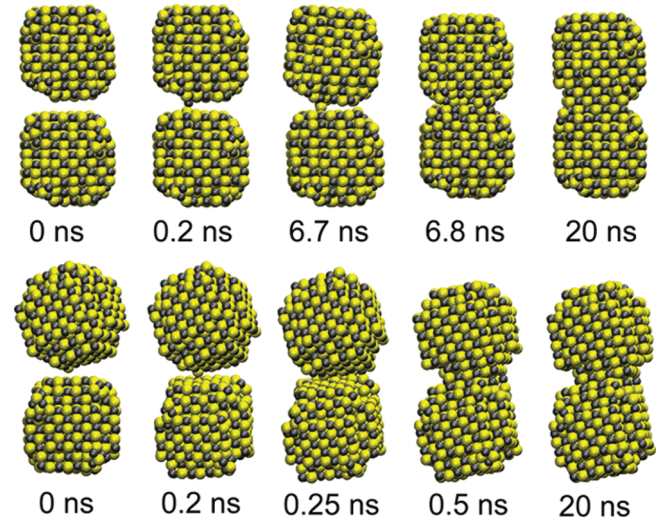

FIGURE 3. Fusion of bare NCs from MD simulations. Top: The NCs are initially {100} facet-to-facet aligned. Bottom: The NCs have an initial mistilt in two directions of 27 and 11°, respectively. Full animations (Movies M1, M2) can be found in the Supporting Information.

We have computed the electrical dipole moment during the various simulations. It has a rather small magnitude (in the order of 50 D) and has no permanent direction with respect to the NC orientation. This electric dipole is induced by thermal displacements of individual ions and by surface defects and is fluctuating randomly at the same time scale as the atomic displacements. Therefore, the chainlike alignment of PbSe NCs in solution, as observed by means of cryo-TEM,[15] is unlikely to be the result of an orientation directed by permanent NC dipoles.

In order to study the alignment and fusion into detail, we have also simulated the attachment and fusion of nanocrystals at 450 K, whereby again the conditions of a TEM experiment[16] are mimicked. A pair of annealed NCs is positioned at a surface-to-surface distance of ∼0.5 nm at a certain mutual orientation, and a MD simulation of 20 ns is conducted. Figure 3 (top) and Supporting Information Movie 1 show the evolution of a pair of NCs in an aligned {100} facet-to-facet orientation. Already after 200 ps, an atomic bridge forms between the two surfaces, along which atoms move back and forth. This bridge persists for a few nanoseconds. During this time, the gap between the two surfaces gradually becomes smaller, until the actual fusion begins after 6.5 ns whereby the gap is closed in two swift movements. First, the two NCs spontaneously tilt to bring their edges into contact. Second, the two NCs tilt back again to close the gap, whereby a defective interface (with a dislocation half-plane) is formed. These interface defects are then healed during the remaining simulation time so that full crystal fusion is achieved.

In the simulations, we have also studied the situation where the NCs have an initial mistilt of 27°/11° in two

DOI: 10.1021/nl101793b | *Nano Lett.* **2010,** *10,* 3966–3971

directions. Figure 3 (bottom) and Supporting Information Movie 2 show the fusion for such a configuration. First, the NCs rotate to bring their surfaces into contact. The mistilt angle increases substantially, up to 35°, during this step. Second, the two NCs rotate back to close the gap and two align the two crystal lattices. No atomic bridges are observed in this case. The fusion itself is a spontaneous process and occurred only in a few simulations due to the limited simulation time. We did not observe NC fusion in simulations with ligands present, but we expect this to be a purely kinetic effect, that is, the fusion is likely to happen after longer simulation times. It has previously been shown[34] that the energetic fusion barrier caused by ligands disappears already after the removal of 15% of the maximum coating. The fusion of the ionic PbSe NCs occurring via direct attachment of planar surfaces is very different from the fusion process of, for example, Au nanoparticles, which occurs through the growth of a bottleneck.[35]

The fusion of PbSe NCs via swift rotations is in excellent agreement with the earlier HRTEM study[16] where it was shown that rotations of the NCs over multiple axes enable crystal unification. During these in situ experiments, the fusion process took place in seconds or minutes rather than in nanoseconds. Apart from the different nanocluster size (small nanocrystals move more easily than larger nanocrystals), this difference is most likely due to the more complicated experimental situation; in a hexagonal array, every NC is surrounded by six other NCs, which also interact with the NC under consideration. Moreover, also the substrate (SiN membrane) and the beam-induced presence of carbon contamination may have an influence on the fusion kinetics. In addition to the nanocrystal rotations, also the interface relaxation is a feature of the fusion process that is confirmed by the simulations. More importantly, these simulations reveal that fusion can happen very efficiently in the absence of permanent dipole−dipole interactions (as discussed previously, the NC electric dipoles were small, variable, and randomly oriented), and therefore it can be concluded that reduction of surface energy constitutes the main driving force for the fusion process.

The question now arises, though, why under certain experimental conditions PbSe NCs align to form nanowires. If surface energy is the only driving force, crystal fusion into three-dimensional structures can be expected, indeed. Here we should remark that very recently, the formation of extended 2D sheets by attachment of PbS nanocrystals in a suspension has been reported.[36] In addition, during the in situ heating TEM experiment[16] performed with dropcasted NCs, the nanocrystals fused into two-dimensional nanocrystals on the two-dimensional support. However, in other experimental investigations,[7,8,14] efficient formation of one-dimensional nanowires has been reported. It is thus clear that the self-organization of the Pb-chalcogenide nanocrystals leads to a wide variety of isotropic and anisotropic architectures, and that subtle changes in the surface chemistry may have strong effects. Several factors may induce dipole moments or promote in another way the one-dimensional alignment of nanocrystals. In the current simulations, the PbSe nanocrystals are stoichiometric, while experimentally it has been found that PbSe NCs can also be off-stoichiometric and deficient in Se.[37,38] Furthermore, both in the current simulations and in the mimicked TEM experiments, only alkylamines are considered as capping molecules, while in the literature the more polar oleic acid capping molecules are often used.

The atomic bridge shown in Figure 3 (top) was observed a few times during the simulations, however the formation of the bridges could not be directly correlated with crystal fusion, as in most cases the formation of a bridge did not result in fusion (within the simulation times). We also have experimental evidence that such bridges occur in reality. Supporting Information Movie M3 shows a real-time TEM recording, whereby a thin, crystalline bridge is connecting two NCs (although in this case, the bridge is present on top of the SiN membrane support and not suspended in vacuum). This recording shows that the bridge can grow and shrink and is often disrupted by the lateral motion of the PbSe NCs at both ends. Although similar experimental observations were made more often, it is usually difficult to distinguish between atomic bridges and fringes on the membrane, contamination caused by carburization of the ligands, etc. The bridge shown in Supporting Information Movie M3 however displays very clearly the PbSe rocksalt lattice.

In summary, a classical interaction potential for PbSe was developed, which very well reproduces the bulk properties of this material. This potential was employed to perform molecular dynamics simulations of nanocrystal fusion and morphological transformations. It is found that two PbSe nanocrystals at close proximity fuse within nanoseconds via direct surface attachment, even for different initial orientations. Crystal fusion occurs via direct attachment of planar surfaces, realized by small, swift rotations, reorientation and interfacial relaxation. In sharp contrast to the general belief, interparticle dipole−dipole interactions were found not to play a significant role in this "oriented attachment" process of stoichiometric PbSe nanocrystals. Using evidence from experiments and simulation, it is shown that atomic bridges occur between the surfaces of adjacent PbSe NCs. These bridges require further investigation to asses their stability, the underlying physical mechanism and potential functionalities. Furthermore, it was found that surfactant-capped, multifaceted nanocrystals do not have fully polar {111} facets, as in thermal equilibrium they are not purely Pb- or Se-terminated. Upon removal of surfactants, all facets different from {100} reconstruct into {100}-terminated fringes within nanoseconds. This reconstruction is in excellent agreement with earlier electron microscope and first-principles studies.

DOI: 10.1021/nl101793b | *Nano Lett.* **2010,** *10,* 3966–3971

Acknowledgment. T.J.H.V. acknowledges financial support from The Netherlands Organization for Scientific Research (NWO—CW) through a VIDI grant. We thank Dr. Changming Fang (TU Delft) for help with the interpretation of DFT calculations.

Supporting Information Available. The Supporting Information contains the fitted potential parameters for PbSe, details of the MD and MC calculations, and three Supporting Movies (M1—M3). This material is available free of charge via the Internet at http://pubs.acs.org.

REFERENCES AND NOTES

(1) Yin, Y.; Alivisatos, A. P. *Nature* **2005**, *437*, 664–670.
(2) Murray, C. B.; Kagan, C. R.; Bawendi, M. G. *Science* **1995**, *270*, 1335–1338.
(3) Talapin, D. V.; Murray, C. B. *Science* **2005**, *310*, 86–89.
(4) Vanmaekelbergh, D.; Liljeroth, P. *Chem. Soc. Rev.* **2005**, *34*, 299–312.
(5) Shevchenko, E. V.; Talapin, D. V.; Kotov, N. A.; O'Brien, S.; Murray, C. B. *Nature* **2006**, *439*, 55–59.
(6) Lifshitz, E.; et al. *Nano Lett.* **2003**, *3*, 857–862.
(7) Tang, Z.; Kotov, N. A.; Giersig, M. *Science* **2002**, *297*, 237–240.
(8) Talapin, D. V.; et al. *J. Phys. Chem. C* **2007**, *111*, 13244–13249.
(9) Nozik, A. J. *Nat. Nanotechnol.* **2009**, *4*, 548–549.
(10) Konstantatos, G.; Howard, I.; Fischer, A.; Hoogland, S.; Clifford, J.; Klem, E.; Levina, L.; Sargent, E. H. *Nature* **2006**, *442*, 180–183.
(11) Sukhovatkin, V.; Hinds, S.; Brzozowski, L.; Sargent, E. H. *Science* **2009**, *324*, 1542–1544.
(12) Choi, J. J.; et al. *Nano Lett.* **2009**, *9*, 3749–3755.
(13) Kang, M. S.; Lee, J.; Norris, D. J.; Frisbie, C. D. *Nano Lett.* **2009**, *9*, 3848–3852.
(14) Cho, K.-S.; Talapin, D. V.; Gaschler, W.; Murray, C. B. *J. Am. Chem. Soc.* **2005**, *127*, 7140–7147.
(15) Houtepen, A. J.; Koole, R.; Vanmaekelbergh, D.; Meeldijk, J.; Hickey, S. G. *J. Am. Chem. Soc.* **2006**, *128*, 6792–6793.
(16) Van Huis, M. A.; Kunneman, L. T.; Overgaag, K.; Xu, Q.; Pandraud, G.; Zandbergen, H. W.; Vanmaekelbergh, D. *Nano Lett.* **2008**, *8*, 3959–3963.
(17) Zhang, Q.; Liu, S.-J.; Yu, S.-H. *J. Mater. Chem.* **2009**, *19*, 191–207.
(18) Talapin, D. V.; Shevchenko, E. V.; Murray, C. B.; Titov, A. V.; Král, P. *Nano Lett.* **2007**, *7*, 1213–1219.
(19) Klokkenburg, M.; Houtepen, A. J.; Koole, R.; de Folter, J. W. J.; Erné, B. H.; van Faassen, E.; Vanmaekelbergh, D. *Nano Lett.* **2007**, *7*, 2931–2936.
(20) Fang, C. M.; van Huis, M. A.; Vanmaekelbergh, D.; Zandbergen, H. W. *ACS Nano* **2010**, *4*, 211–218.
(21) Rabani, E. *J. Chem. Phys.* **2002**, *116*, 258–262.
(22) Rabani, E. *J. Chem. Phys.* **2001**, *115*, 1493–1497.
(23) Schapotschnikow, P.; Hommersom, J.; Vlugt, T. J. H. *J. Phys. Chem. C* **2009**, *113*, 12690–12698.
(24) Wick, C. D.; Stubbs, J. M.; Rai, N.; Siepmann, J. I. *J. Phys. Chem. B* **2005**, *109*, 18974.
(25) Gale, J. D. *J. Chem. Soc., Faraday Trans.* **1997**, *93*, 629.
(26) Gale, J. D.; Rohl, A. L. *Mol. Simul.* **2003**, *29*, 291.
(27) Hummer, K.; Grüneis, A.; Kresse, G. *Phys. Rev. B* **2007**, *75*, 195211.
(28) Chattopadhyay, T.; von Schnering, H. G.; Grosshans, W. A.; Holzapfel, W. B. *Physica B+C* **1986**, *139—140*, 356–360.
(29) Mariano, A. N.; Chopra, K. L. *Appl. Phys. Lett.* **1967**, *10*, 282–284.
(30) Ahuja, R. *Phys. Status Solidi B* **2003**, *235*, 341–347.
(31) Lach-hab, M.; Papaconstantopoulos, D. A.; Mehl, M. J. *J. Phys. Chem. Solids* **2002**, *63*, 833–841.
(32) Wei, S.-H.; Zunger, A. *Phys. Rev. B* **1997**, *55*, 13605.
(33) Semiconductors: Group IV Elements, IV-IV and III-V Compounds. *Landolt-Börnstein, New Series*; Springer: Berlin, 2005; Vol 41.
(34) Schapotschnikow, P.; Pool, R.; Vlugt, T. J. H. *Nano Lett.* **2008**, *8*, 2930–2934.
(35) Lim, T. H.; McCarthy, D.; Hendy, S. C.; Stevens, K. J.; Brown, S. A.; Tilley, R. D. *ACS Nano* **2009**, *3*, 3809–3813.
(36) Schliehe, C.; Juarez, B. H.; Pelletier, M.; Jander, S.; Greshnykh, D.; Nagel, M.; Meyer, A.; Foerster, S.; Kornowski, A.; Klinke, C.; Weller, H. *Science* **2010**, *329*, 550–553.
(37) Moreels, I.; Fritzinger, B.; Martins, J. C.; Hens, Z. *J. Am. Chem. Soc.* **2008**, *130*, 15081–15086.
(38) Petkov, V.; Moreels, I.; Hens, Z.; Ren, Y. *Phys. Rev. B* **2010**, *81*, 241304.

DOI: 10.1021/nl101793b | *Nano Lett.* **2010,** *10,* 3966--3971